



THE UNIVERSITY *of* EDINBURGH

Edinburgh Research Explorer

Tissue-Specific Expression of FLOWERING LOCUS T in Arabidopsis Is Maintained Independently of Polycomb Group Protein Repression

Citation for published version:

Farrona, S, Thorpe, FL, Engelhorn, J, Adrian, J, Dong, X, Sarid-Krebs, L, Goodrich, J & Turck, F 2011, 'Tissue-Specific Expression of FLOWERING LOCUS T in Arabidopsis Is Maintained Independently of Polycomb Group Protein Repression' *The Plant Cell*, vol. 23, no. 9, pp. 3204-3214. DOI: 10.1105/tpc.111.087809

Digital Object Identifier (DOI):

[10.1105/tpc.111.087809](https://doi.org/10.1105/tpc.111.087809)

Link:

[Link to publication record in Edinburgh Research Explorer](#)

Document Version:

Publisher's PDF, also known as Version of record

Published In:

The Plant Cell

Publisher Rights Statement:

Open Access Article

General rights

Copyright for the publications made accessible via the Edinburgh Research Explorer is retained by the author(s) and / or other copyright owners and it is a condition of accessing these publications that users recognise and abide by the legal requirements associated with these rights.

Take down policy

The University of Edinburgh has made every reasonable effort to ensure that Edinburgh Research Explorer content complies with UK legislation. If you believe that the public display of this file breaches copyright please contact openaccess@ed.ac.uk providing details, and we will remove access to the work immediately and investigate your claim.



Tissue-Specific Expression of *FLOWERING LOCUS T* in *Arabidopsis* Is Maintained Independently of Polycomb Group Protein Repression

Sara Farrona,^a Frazer L. Thorpe,^b Julia Engelhorn,^a Jessika Adrian,^{a,1} Xue Dong,^a Liron Sarid-Krebs,^a Justin Goodrich,^b and Franziska Turck^{a,2}

^aMax Planck Institute for Plant Breeding Research, 50829 Cologne, Germany

^bInstitute for Molecular Plant Sciences, University of Edinburgh, Edinburgh EH9 3JH, United Kingdom

The Polycomb Group (PcG) pathway represses transcription through a mechanism conserved among plants and animals. PcG-mediated repression can determine spatial territories of gene expression, but it remains unclear whether PcG-mediated repression is a regulatory requirement for all targets. Here, we show the role of PcG proteins in the spatial regulation of *FLOWERING LOCUS T (FT)*, a main activator of flowering in *Arabidopsis thaliana* exclusively expressed in the vasculature. Strikingly, the loss of PcG repression causes down-regulation of *FT*. In addition, our results show how the effect of PcG-mediated regulation differs for target genes and that, for *FT* expression, it relies primarily on tissue differentiation.

INTRODUCTION

Two main complexes are involved in the repression mediated by the Polycomb Group (PcG) pathway. Polycomb Repressive Complex2 (PRC2) tri-methylates lysine 27 of histone 3 (H3K27me3) and recruits PRC1, which further contributes to the repression of target genes (Hennig and Derkacheva, 2009; Simon and Kingston, 2009). The expression of homeotic (Hox) genes is the paradigm of PcG regulation in animals. Hox genes are expressed only in specific regions of the animal body; however, in PcG mutants their expression extends to other regions, causing homeotic changes in body patterning (Simon and Kingston, 2009). In plants, the best known example of a Hox gene spatially regulated by PcG proteins is the *Arabidopsis thaliana* MADS box gene *AGAMOUS (AG)*. In the wild-type plants, *AG* is expressed only in the flowers, whereas in PcG mutants, it is ectopically expressed in leaves and other parts of the plant, correlating with a decrease in H3K27me3 (Goodrich et al., 1997; Chanvivattana et al., 2004; Schubert et al., 2006; Calonje et al., 2008). H3K27me3 target genes in *Arabidopsis* often show marked tissue-specific expression patterns (Turck et al., 2007; Zhang et al., 2007). Two recent tissue-specific, genome-wide distribution studies of H3K27me3 have revealed that the H3K27me3 is mostly absent from targets in the tissues where these are expressed (Weinhofer et al., 2010; Lafos et al., 2011). On the other hand, changes in H3K27me3 levels are not always

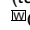
correlated with changes in transcription (Schubert et al., 2006; Schwartz and Pirrotta, 2007; Kwon et al., 2009; Adrian et al., 2010).

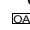
H3K27me3 is widely dispersed across the *FLOWERING LOCUS T (FT)* locus (Turck et al., 2007; Zhang et al., 2007), and the histone mark is proposed to delimit the accessibility of transcription factors to certain *cis*-elements at the *FT* promoter (Adrian et al., 2010). Chromatin-mediated repression is required to confer photoperiod-dependent control of *FT* expression (Goodrich et al., 1997; Takada and Goto, 2003). *FT* encodes a plant florigen and is induced by long-day conditions through the activator CONSTANS (CO) (Turck et al., 2008; Imaizumi, 2010). CO has been shown to bind DNA sequences specifically *in vitro*, and CO consensus binding sites within the proximal *FT* promoter are functional *cis*-elements required for *FT* expression (Adrian et al., 2010; Tiwari et al., 2010). However, these elements and the proximal promoter alone are not sufficient to drive expression of reporter genes in transgenic plants, but require the presence of enhancer elements that are located more than 4 kb from the transcription start (Adrian et al., 2010). One striking aspect of *FT* transcriptional regulation is its spatial pattern: prior to flowering, *FT* is expressed only in the phloem companion cells of the cotyledons and the distal blade of rosette leaves (Takada and Goto, 2003; Yamaguchi et al., 2005; Adrian et al., 2010); after flowering, the gene is also expressed in other organs (cauline leaves, sepals, and fruits) but is still strongly limited to the vascular tissue (Adrian et al., 2010). *FT* expression is limited to the vasculature even if CO is provided ectopically (Yamaguchi et al., 2005; Adrian et al., 2010). In plants carrying mutations in *LIKE HETEROCHROMATIN PROTEIN1 (LHP1)*, a *FT* expression pattern similar to that of CO-overexpressing plants is observed (Takada and Goto, 2003). LHP1 directly represses *FT* as part of a plant PRC1, but in *lhp1* mutants the PcG pathway is only partially affected, and the level of H3K27me3 at *FT* does not change (Turck et al., 2007; Farrona et al., 2008); therefore, the analysis

¹ Current address: Department of Biological Sciences, Stanford University, Stanford, California 94305.

² Address correspondence to turck@mpipz.mpg.de.

The author responsible for distribution of materials integral to the findings presented in this article in accordance with the policy described in the Instructions for Authors (www.plantcell.org) is: Franziska Turck (turck@mpipz.mpg.de).

 Online version contains Web-only data.

 Open Access articles can be viewed online without a subscription. www.plantcell.org/cgi/doi/10.1105/tpc.111.087809

of this mutant is not sufficient to understand the role of PcG proteins in *FT* regulation. As neither CO nor LHP1 are responsible for the characteristic tissue-specific expression pattern of *FT*, other regulatory components must be involved.

Here we investigate whether the H3K27me3 mark is required for the tissue-specific expression pattern of *FT* as part of a PcG-mediated repression mechanism that is independent of LHP1. We show that the loss of PcG repression differentially affects targets, and that the domain of *FT* expression depends on tissue differentiation, even in the absence of a PcG-mediated chromatin configuration.

RESULTS

FT Expression Is Strongly Reduced in the *swn-7 clf-28* PcG Mutant

To analyze PcG-mediated *FT* spatial expression, a transgene carrying an 8.1-kb *FT* promoter fragment fused to the β -Glucuronidase gene (*FT_{prom}:GUS*) (Adrian et al., 2010) was introduced into the single *clf-28* (*clf*) and double *swn-7 clf-28* (*swn clf*) PcG

mutants (Figure 1). CURLY LEAF (CLF) and SWINGER (SWN) are part of the histone methyltransferase SET family responsible for H3K27me3 deposition. CLF and SWN show partially overlapping functions and are involved in *FT* repression (Jiang et al., 2008; Liu et al., 2010). In the wild-type plants, the *FT_{prom}:GUS* signal was obtained only at the vascular tissue of cotyledons and leaves, as expected (Figures 1A and 1D) (Takada and Goto, 2003; Adrian et al., 2010). In *clf* mutant plants, the signal was stronger (Figures 1B and 1E), which supported the quantitative RT-PCR (qRT-PCR) data (Figure 2A) (Barrero et al., 2007; Jiang et al., 2008), but it was still limited to the vascular tissue. Mutant seeds of *swn clf* germinate, giving rise to a small seedling that degenerates to a callus-/embryo-like structure (Chanvivattana et al., 2004). In *swn clf* seedlings, the *FT* signal was observed at the veins of cotyledons and in leaf-like structures (Figures 1C and 1F). In addition, the roots are also stained, and a strong, diffused signal is observed at the hypocotyls. Strikingly, as the tip of the root develops a swollen and opaque embryo-like tissue, known as a pickle (pk1)-like root phenotype (Ogas et al., 1997), *FT* promoter-driven signal completely disappears (Figure 1F). In 2-month-old *swn clf* callus, the GUS signal strongly decreased and was obtained only in a punctate pattern (Figure 1G). Expression

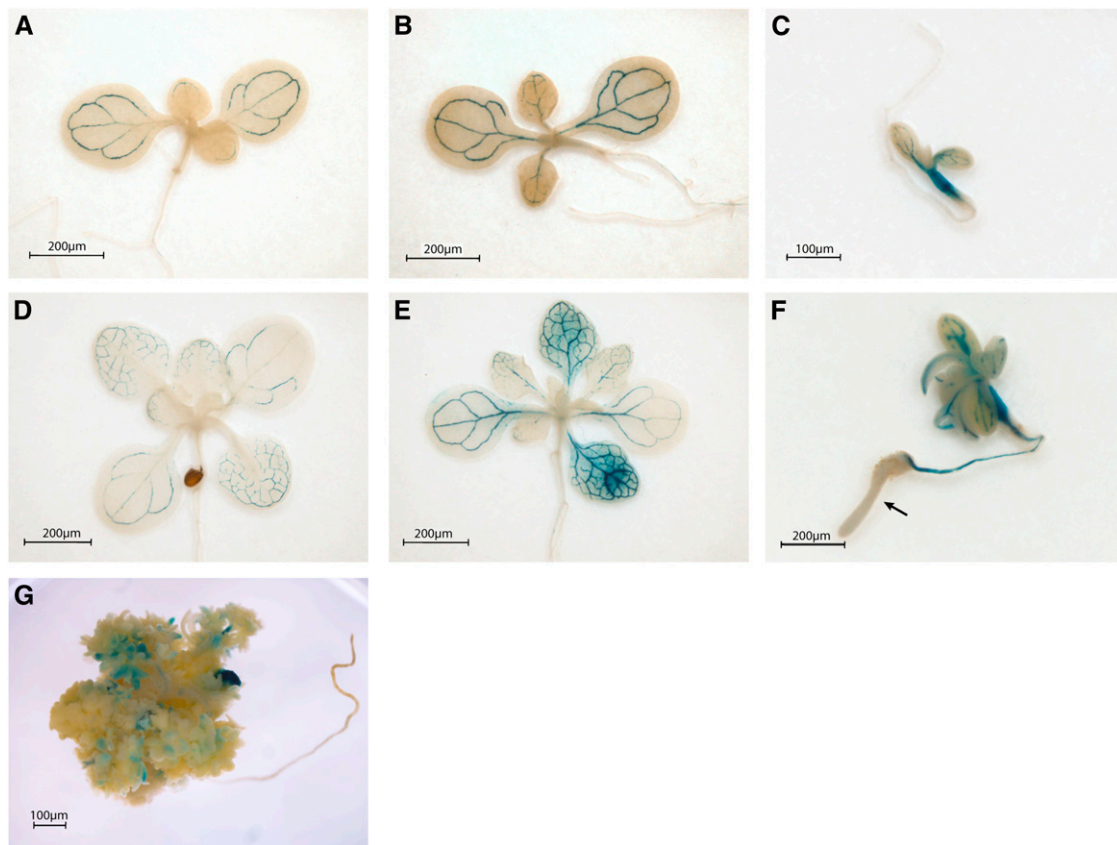


Figure 1. *FT* Spatial Expression Changes in the Wild Type, *clf*, and *swn clf*.

(A) to (G) Histochemical localization of GUS activity in 10- and 20-day-old wild-type, *clf*, and *swn clf* seedlings and 2-month-old *swn clf* callus carrying an *FT_{prom}:GUS* construct. Ten-day-old wild type (A), *clf* (B), and *swn clf* (C); 20-d-old wild type (D), *clf* (E), and *swn clf* (F); 2-month-old *swn clf* (G). Arrow in (F) indicates the loss of GUS signal in the pk1-like root.

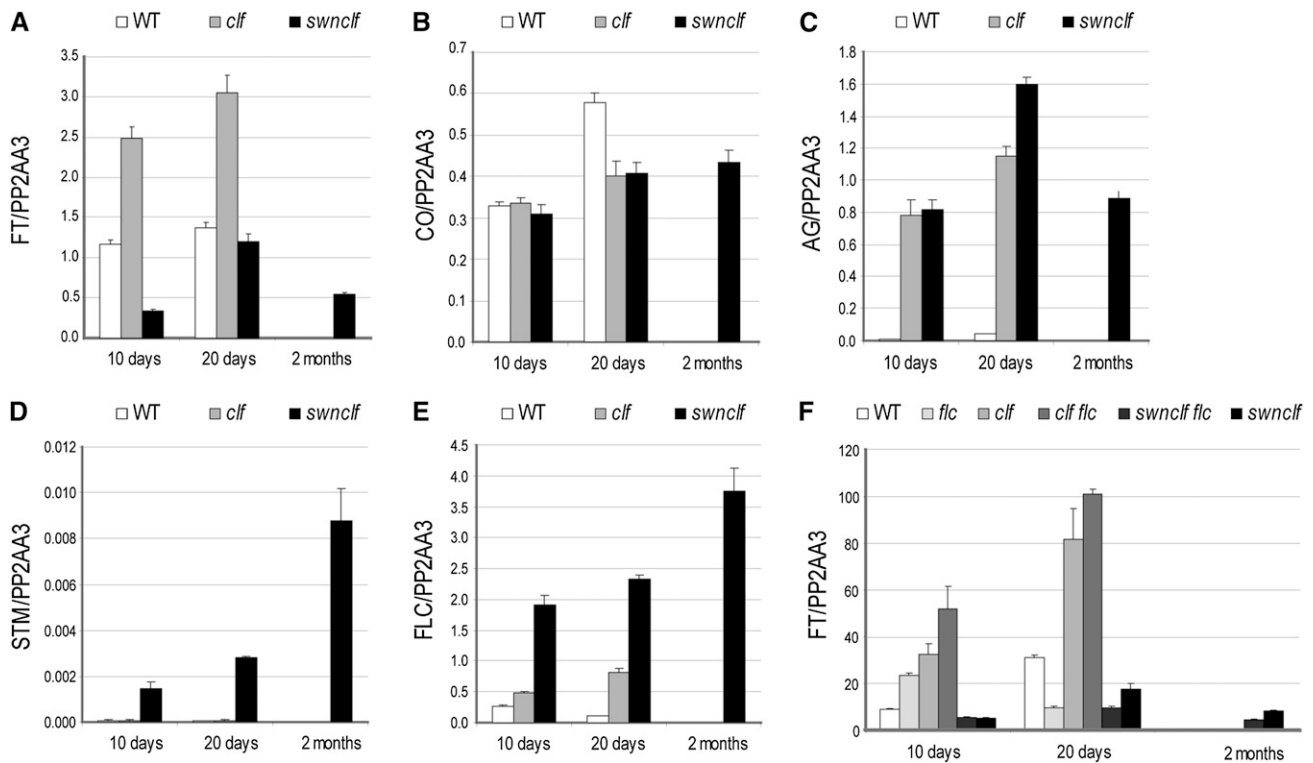


Figure 2. Expression Analysis in the Wild Type, *clf*, and *swncf*.

(A) to (E) qRT-PCRs in 10- and 20-d-old wild type (WT), *clf*, and *swncf* and 2-month-old *swncf* callus. qRT-PCRs of *FT* (A), *CO* (B), *AG* (C), *STM* (D), and *FLC* (E).

(F) qRT-PCRs of *FT* in 10- and 20-d-old wild type, *flc*, *clf*, *clf flc*, *swncf flc*, and *swncf* and 2-month-old *swncf flc* and *swncf* callus.

Error bars represent SE of the mean based on three technical replicates. Similar results were obtained in at least two independent experiments. A biological replicate of the analysis is included as Supplemental Figure 6 online.

analysis confirmed a reduction in *FT* in *swncf* (Figure 2A) despite a maintained expression of *CO* (Figure 2B). By contrast, *AG* is strongly expressed in *clf* and *swncf* mutants, indicating that its regulation depends mostly on CLF; whereas *STM* is up-regulated only in the *swncf* background and, therefore, is more dependent on SWN (Figures 2C and 2D) (Schubert et al., 2006).

To further characterize the expression pattern of other PcG targets and to investigate whether other genes mimic *FT* expression in PcG mutants, the expression of H3K27me3-enriched genes in the wild type, *clf*, and *swncf* was analyzed by expression microarray analysis and clustered according to the different patterns of expression. Although an important percentage of PcG targets was strongly up-regulated in *swncf* plants, the clustering showed that *FT*, which is placed in cluster 1, is not an exception among PcG target genes, because 9.7% of all H3K27me3-enriched genes follow a similar pattern of expression. In addition, other clusters showed only slight expression changes between the wild-type and mutant plants (Figure 3; see Supplemental Figure 1 and Supplemental Data Set 1 online).

In summary, despite the general role of PcG in establishing a repressive chromatin configuration and thereby participating in tissue-specific gene regulation, loss of PcG repression is not synonymous with transcriptional activation, and no general rule predicts how expression might change in PcG mutants.

***FLC* Overexpression Is Not the Cause of *FT* Repression in the *swncf* Mutant**

The MADS box transcription factors FLOWERING LOCUS C (*FLC*) and SHORT VEGETATIVE PHASE (*SVP*) directly repress *FT* (Li et al., 2008), and the expression of *FLC* itself is regulated by CLF and SWN as part of different PRC2 complexes (Hennig and Derkacheva, 2009; Liu et al., 2010). Like *FLC*, the *SVP* locus is covered by the H3K27me3 mark, indicating repression by PcG proteins, although such regulation has not been described (Zhang et al., 2007). *FLC* was up-regulated in *clf* plants compared with the wild-type plants (Figure 2E) (Jiang et al., 2008) and was further increased in *swncf* plants, indicating that *FLC* repression depends on both PcG proteins (Figure 2E). By contrast, *SVP* is not up-regulated in *clf* or *swncf* plants (see Supplemental Figure 2A online). AP2-like proteins TEMPRANILLO1 (*TEM1*), *TEM2*, and SCHLAFMÜTZE (*SMZ*) repress *FT* expression (Imazumi, 2010) but are not marked by H3K27me3 and are down-regulated in *swncf* (see Supplemental Figures 2B to 2D online). Therefore, *FLC*, but neither *SVP* nor *TEM1* and 2 or *SMZ*, might cause *FT* down-regulation in *swncf*. To investigate the role of *FLC*, *FT* expression was analyzed in the triple mutant *swncf-7 clf-28 flc-3* (*swncf flc*). Although loss of *FLC* caused an increase in *FT* expression in the *clf* mutant, no up-regulation was observed in

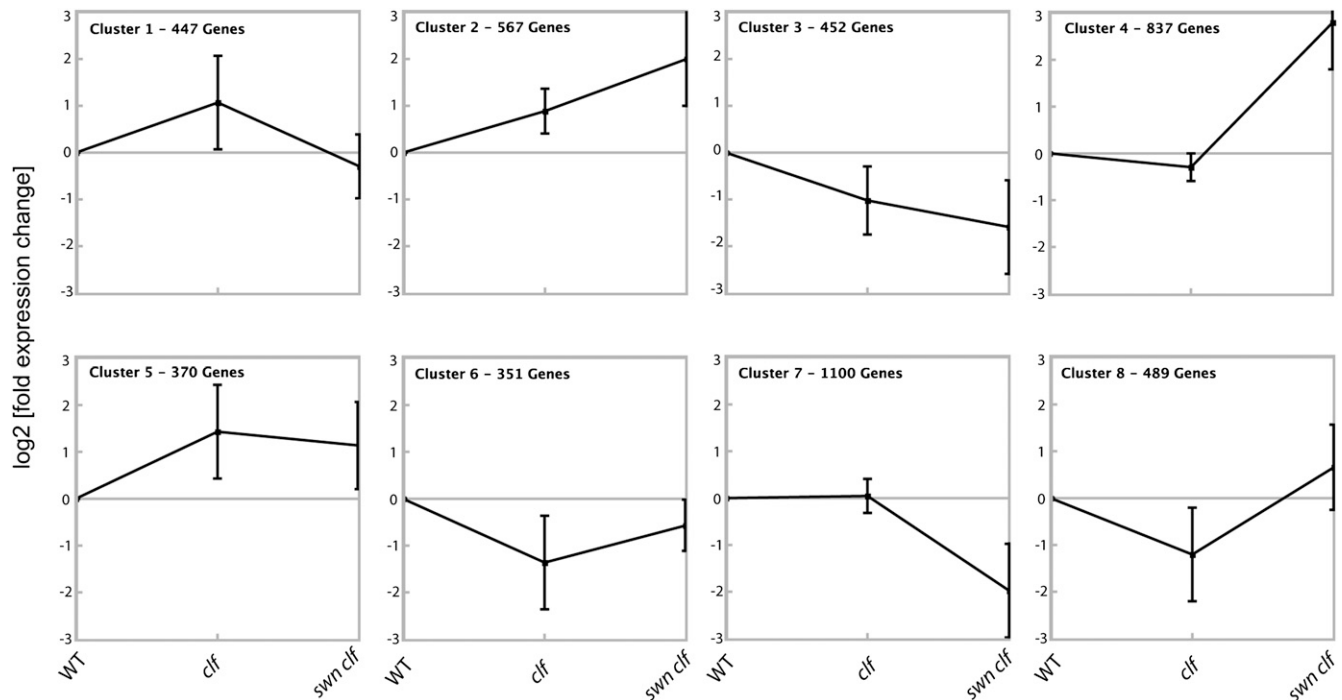


Figure 3. K-Means Clustering of Expression Data of H3K27me3-Enriched Genes in PcG Mutant Seedlings.

The expression data of the H3K27me3-enriched set of genes ($n = 4599$) were analyzed by K-means clustering ($k = 8$) using the software Genesis. Expression values for each gene were calculated as fold change compared with the wild type (WT). Clustering was performed on log₂-transformed fold-change values. The Pearson correlation coefficient was used as a distance measurement to cluster according to patterns rather than absolute values. Each graph represents one cluster. Squares represent the average expression, and bars indicate the normalized SD. *FT* is located in Cluster 1.

the *swn clf* background (Figure 2F), demonstrating that FLC is not involved in *FT* down-regulation in this genetic background.

Chromatin Changes at *FT* Are Not Sufficient to Explain Its Down-Regulation

FT expression data obtained in *clf* and *swn clf* mutants were correlated to changes in *FT* chromatin (Figure 4A). It has been reported that H3K27me₃ is absent at *FT* in *clf* (Jiang et al., 2008); however, our ChIP data show that this loss is not homogeneous for the whole *FT* locus, because significant enrichment of H3K27me₃ can still be detected at the 3' region. In *swn clf* plants, the H3K27me₃ signal completely disappeared (Figure 4B). LHP1 binding to *FT* followed almost exactly the same pattern as H3K27me₃ in the single and double mutants (Figure 4C). Similar results were obtained for the *AG* locus (see Supplemental Figure 3A online).

Loss of H3K27me₃ and LHP1 promotes a more permissive chromatin structure, which cannot explain the down-regulation of *FT* observed in *swn clf*. Therefore, we analyzed whether, in the absence of H3K27me₃, the repressive histone marks H3K9me₂ and H3K27me₁ were recruited to *FT*. H3K9me₂ ChIP data at *FT* showed some increase of this mark over the *FT* locus only in *swn clf* plants. However, the H3K9me₂ increase at *FT* seems nonsignificant when compared with levels at the Ta3 retrotransposon, although no studies have shown threshold levels for

effective H3K9me₂-mediated repression (Figure 4D). For H3K27me₁, the ChIP data showed an inverse correlation between changes in this mark and H3K27me₃ changes at *FT* (Figures 4B and 4E). An increase in H3K27me₁ was also observed at *AG*, despite the strong up-regulation of this gene in *swn clf* (see Supplemental Figure 3B online).

H3K4me₃ has been shown to act as a bivalent mark together with H3K27me₃ at the *FT* and *FLC* loci (Jiang et al., 2008; Carles and Fletcher, 2009). Increased H3K4me₃ levels were reported in the 5' region of *FT* and *AG* in the *clf* mutant (Carles and Fletcher, 2009). Our ChIP experiments did not show any significant changes for H3K4me₃ in the *clf* background either at *FT* or *AG* (see Supplemental Figures 3C and 3D online). An increase for this mark was observed in *swn clf* plants, despite the repression of *FT* (see Supplemental Figure 3D online).

In conclusion, despite their divergent expression, *FT* and *AG* are subjected to similar changes in chromatin conformation in the PcG mutants. Therefore, chromatin changes are not sufficient to explain *FT* down-regulation in *swn clf*.

FT Expression Is Strongly Reduced upon Loss of Vascular Identity in Induced Callus

In *swn clf* plants, development of the vascular tissue is particularly affected. The characteristic reticulated pattern of the veins is lost in the leaf-like structures, and the linear pattern is

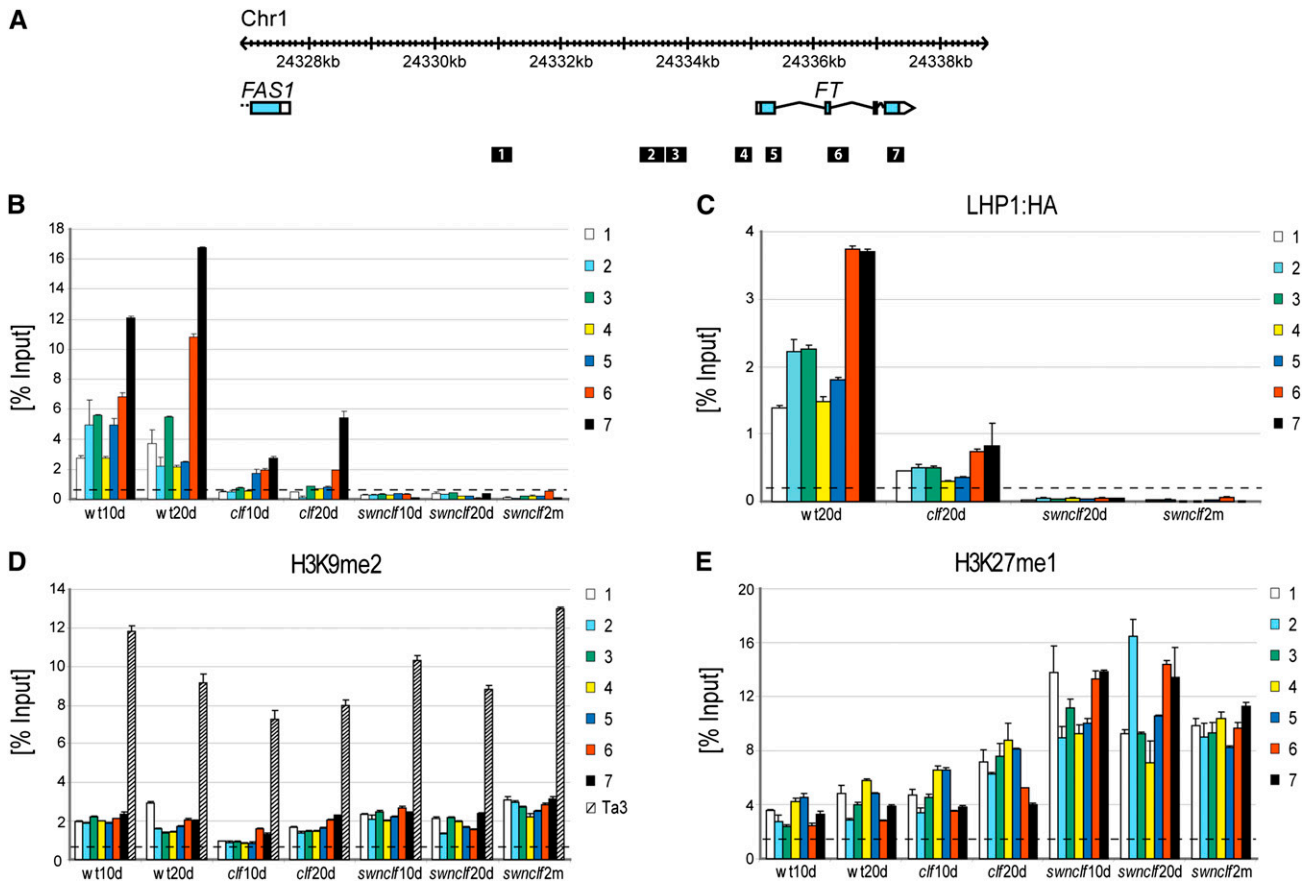


Figure 4. Chromatin Changes at *FT* in the Wild Type, *clf*, and *swn clf*.

(A) Genome browser view of the *FT* locus at chromosome 1. Exons of *FT* and upstream gene *FAS1* are represented as blue boxes, and untranslated regions are represented as white boxes. Positions of amplicons used in the ChIP analysis are presented as black boxes and are numbered.

(B) H3K27me3 at *FT* locus. ChIP experiments were performed with chromatin from 10-d-old (10d) and 20-d-old (20d) wild type (wt), *clf*, and *swn clf* and 2-month-old (2m) *swn clf* plants. Signals detected along the *FT* locus were normalized against the input.

(C) Binding of LHP1 at *FT* locus. ChIP experiments were performed with chromatin from 20-d-old (20d) wild type, *clf*, and *swn clf* and 2-month-old (2m) *swn clf* plants carrying a $35S_{prom}:LHP1:HA$ transgene. Normalization as in **(B)**.

(D) H3K9me2 at *FT* locus and the Ta3 retrotransposon. Data are based on the same chromatin extract and analysis as used in **(B)**.

(E) H3K27me1 at *FT* locus. Data are based on the same chromatin extract and analysis as used in **(B)**.

Error bars represent SE of the mean based on three technical replicates. Dashed lines represent background calculated as average of qPCR signals obtained from each sample with Ta3 primers **(B)** and **(C)** or *RBCS1A* primers **(D)** and **(E)**, as described in Methods. A biological replicate of the analysis is included as Supplemental Figure 7 online.

interrupted in the roots (Figure 1G; see Supplemental Figure 4 online). To analyze the importance of vascular development in the down-regulation of *FT* in *swn clf* calli, the $FT_{prom}:GUS$ line in the wild-type background was germinated on callus-inducing medium. In hormone-induced callus, *FT* was expressed only in the cotyledons (Figure 5A), which are formed during embryogenesis and were therefore less affected by the hormone treatment. In these organs, *FT* was strongly expressed in the veins from where the signal diffused to the surrounding cells (Figure 5B). In the hormone-induced opaque embryo-like tissue that lacked differentiation of veins, the GUS signal disappeared, similar to the results obtained in *pkl*-like roots and callus of the *swn clf* mutant (Figures 1F, 1G, and 5A). The loss of GUS signal in the hormone-induced callus occurred despite a high and ectopic

up-regulation of *CO* (Figure 5C) and the presence of *CO* protein (see Supplemental Figure 5 online). Strong expression of *CO* in the cotyledons might cause high $FT_{prom}:GUS$ signal in these organs in the callus-inducing medium.

We next assessed whether an increase in the number of leaf veins could lead to higher expression of *FT*. 1-*N*-Naphtylphthalamic acid (NPA) affects vascular patterning by inhibiting auxin efflux (Wenzel et al., 2008). NPA treatment increases the number and width of vascular bundles but impairs vein differentiation, because the cells within the vascular strand are improperly aligned and the petiole vessels are not connected to those of the stem (Wenzel et al., 2008). *FT* expression decreased in NPA-treated plants, despite the apparent increase in vasculature (Figure 6).

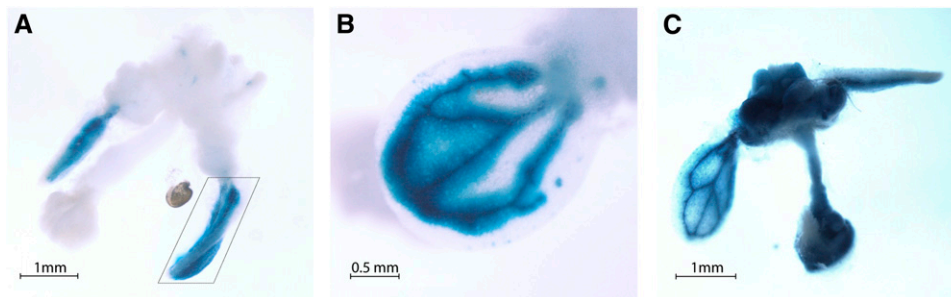


Figure 5. *FT* Spatial Expression in Hormone-induced Callus.

(A) and (B) Histochemical localization of GUS activity in *FT_{prom}:GUS* plants in the wild-type background grown for 10 d on GM medium supplemented with 4.5 μ M 2,4-D and 0.45 μ M kinetin.

(B) Detail of the adaxial surface of the cotyledon marked on (A) with a square.

(C) Histochemical localization of GUS activity in *CO_{prom}:GUS* plants in the wild-type background grown as in (A).

Taken together, the results confirm the necessity of proper vascular development and differentiation to establish the domain of *FT* expression.

DISCUSSION

FT Expression Domain Is Reduced in Strong PcG Mutants

Previous studies have shown the requirement for PcG repression to define territories of expression of different target genes in animals and plants. Consequently, in PcG mutants the expression of such target genes extends to other domains (Goodrich et al., 1997; Chanvivattana et al., 2004; Schubert et al., 2006; Calonje et al., 2008; Simon and Kingston, 2009; Bratzel et al., 2010). We have focused on *FT*, a PcG target with a well-known and defined spatial pattern, to characterize this regulation further. Although in *clf* mutants, *FT* is up-regulated (Figure 2A) (Barrero et al., 2007; Jiang et al., 2008), our results showed that *FT* expression in *clf* is confined to the vascular tissue, its normal domain of expression. However, in calli of the strong PcG double mutant *swn clf*, *FT* domain of expression is not ectopically extended, but rather is strongly reduced to a small group of cells. Clustering analysis of PcG targets divided them in eight different clusters according to their pattern of expression in the wild-type, *clf*, and *swn clf* seedlings. Cluster 2, Cluster 4, Cluster 5, and Cluster 8, with almost 50% of the targets, include genes with a very strong to moderate up-regulation in *swn clf* plants, as expected after the loss of a general repressive pathway. Some targets differentially depend on CLF and SWN (Figure 2) (Schubert et al., 2006). Indeed, Cluster 5 includes genes that depend mainly on CLF, and genes in Cluster 2 depend on both proteins, whereas for genes in Cluster 4, the absence of SWN has a strong effect. Strikingly, \sim 10% of PcG targets show similar regulation as *FT*, with high expression in *clf* and low expression in *swn clf* (Cluster 1). The dependency of *FT* on signals lost in the de-differentiated *swn clf* callus may therefore be a model for the regulation of many PcG targets.

FT down-regulation in *swn clf* could be due to the up-regulation of a repressor. *FT* plays a central role in flowering and, therefore, is tightly regulated by different flowering pathways (Turck et al.,

2008; Imaizumi, 2010). TEM1 and TEM2 are partially overlapping AP2-like transcription factors that repress *FT* directly by binding to the region encoding the 5' untranslated region (Castillejo and Pelaz, 2008). SMZ, which belongs to a different AP2 clade (Aukerman and Sakai, 2003), also represses *FT* expression but interacts with a region several kilobases downstream of the coding region (Mathieu et al., 2009). The MADS box factors FLC and SVP form a complex that represses *FT* transcription, interacting with CArG *cis*-elements located in the first intron and *FT* proximal promoter region (Searle et al., 2006; Li et al., 2008). TEM1, TEM2, and SMZ are not PcG targets, and the microarray analysis showed that these genes are not up-regulated, but rather are down-regulated in *swn clf* plants. Therefore, we discarded them as the potential cause for *FT* down-regulation in *swn clf* plants. SVP is enriched in H3K27me3 but belongs to Cluster 3, which includes genes that are down-regulated in *clf* and *swn clf* plants. The results were confirmed by qRT-PCR, indicating that SVP is probably not involved in *FT* down-regulation in *swn clf* mutants.

FLC is the best characterized PcG target in *Arabidopsis*. Different PcG complexes have been shown to regulate FLC. The VRN-PRC2 complex participates in the vernalization pathway that stably represses FLC after a prolonged exposure to cold temperatures, whereas the EMF-PRC2 complex seems to regulate FLC independently of vernalization (Hennig and Derkacheva, 2009). CLF and SWN are components of both complexes (Hennig and Derkacheva, 2009; Liu et al., 2010). The expression analysis indicated an additive effect of both proteins in FLC regulation, and, therefore, FLC was a candidate for *FT* down-regulation in *swn clf*. However, the genetic data concluded that FLC is not the factor responsible for the decrease in *FT* expression in the strong PcG mutants. Our results do not exclude that other putative repressors could down-regulate *FT* in *swn clf* plants, but the known direct repressors do not have a role in *FT* down-regulation in the absence of PcG regulation.

Chromatin Changes Are Not Key Factors in Determining *FT* Spatial Expression

The PcG pathway modifies chromatin conformation, which is believed to repress transcription by interfering with the binding of

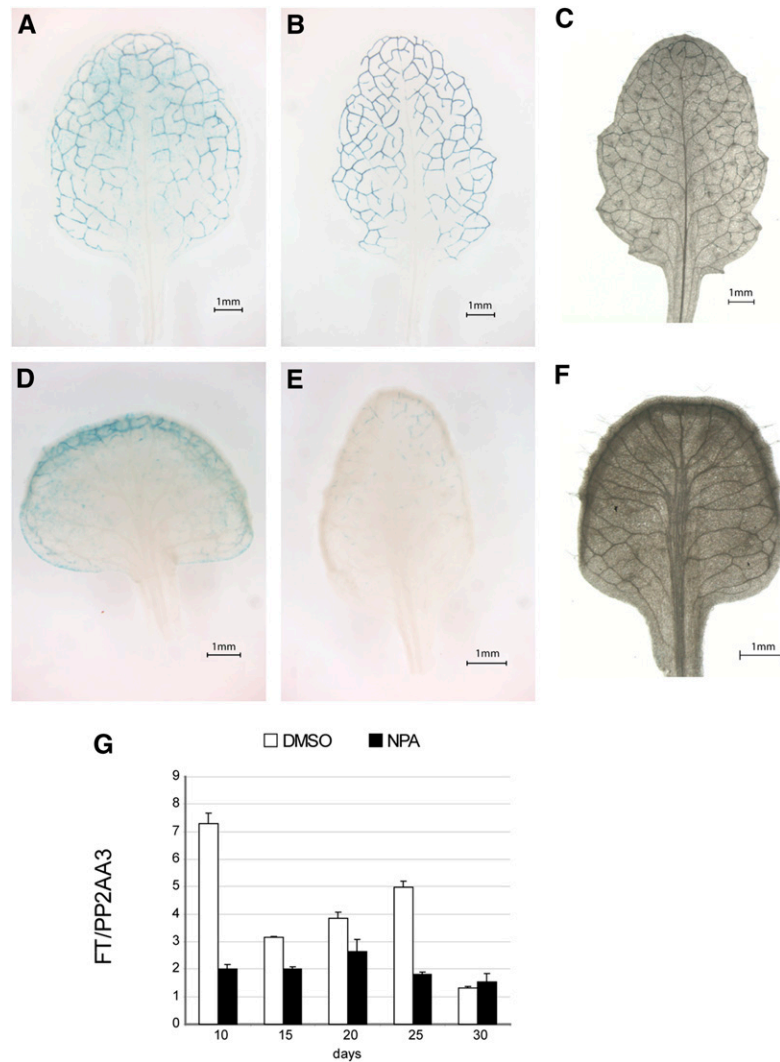


Figure 6. Expression Analysis of *FT* in the Presence of an Auxin Transporter Inhibitor.

(A) and (B) Histochemical localization of GUS activity in leaves of 25-d-old *8.1kbFT_{promi}:GUS* plants grown on GM plates supplemented with DMSO.

(C) Vasculature organization of a 25-d-old leaf grown on GM plates supplemented with DMSO.

(D) and (E) Histochemical localization of GUS activity in leaves of 25-d-old *8.1kbFT_{promi}:GUS* plants grown on GM plates supplemented with NPA.

(F) Vasculature organization of a 25-d-old leaf grown on GM plates supplemented with NPA.

(G) qRT-PCRs in plants grown on GM plates supplemented with DMSO or NPA. Data were normalized to *PP2AA3*. Error bars represent SE of the mean based on three technical replicates.

transcription factors to *cis*-elements, affecting the recruitment of the RNA polymerase and blocking transcriptional initiation and/or elongation (Simon and Kingston, 2009). However, transcription also feeds back on chromatin conformation, and it is not yet fully resolved under which conditions the chromatin plays a determining regulatory role in the regulation of individual target genes (Buzas et al., 2011). Therefore, we investigated whether changes in *FT* and *AG* chromatin correlated with the transcriptional changes observed in *swn clf* plants.

We observed a reduction of H3K27me3 in *clf* at both loci and a complete loss in *swn clf*, pointing out that a SWN-PRC2 complex is also involved in *FT* methylation. LHP1, as part of a PRC1,

recognizes and binds to its targets by direct interaction with the H3K27me3 mark (Exner et al., 2009). It has been suggested that H3K27me3 contributes to, but is not fully responsible for, PRC1 targeting (Simon and Kingston, 2009). Our data showed that LHP1 binding mirrors H3K27me3 occurrence, and, therefore, that at *FT* and *AG*, H3K27me3 acts as obligatory docking site for LHP1.

In the absence of the PcG signatures H3K27me3 and LHP1, other repressive marks could be recruited and spread over the *FT* locus. In *Arabidopsis*, H3K9me2 is a repressive mark characteristic of heterochromatic regions that is excluded from H3K27me3-enriched regions (Turck et al., 2007). Although the minimum level of H3K9me2 required to promote

down-regulation is unknown, the slight increase in this mark observed at *FT* in *swn clf* mutants seems nonsignificant when compared with the H3K9me2 levels at the Ta3 retrotransposon. Consequently, we do not favor a role for H3K9me2 in *FT* down-regulation. H3K27me1 is also considered as a repressive histone mark and is believed to be the precursor for H3K27me3 (Campos and Reinberg, 2009). In *Arabidopsis*, a decrease in H3K27me3 does not affect nuclear H3K27me1 levels (Lafos et al., 2011). We did observe local increase in H3K27me1, but, considering that similar changes in H3K27me1 were observed at *FT* and *AG* (Figure 4; see Supplemental Figure 3 online), this mark neither predicts nor follows the transcriptional state in *swn clf* plants. Because H3K27me1 reflects the reduced activity of PRCs, it might also be a PRC2 substrate in *Arabidopsis*.

H3K4me3 is part of the active Trithorax Group pathway, which antagonizes PcG regulation (Köhler and Hennig, 2010). In animal stem cells, active and repressive chromatin marks are present at the same developmental loci and poise their targets for activation or repression during differentiation (Fisher and Fisher, 2011). In *Arabidopsis*, bivalent chromatin was demonstrated for *FT* and *FLC* (Jiang et al., 2008), and a role of bivalent chromatin in fine-tuning *FLC* and *FT* expression was suggested (Jiang et al., 2008; Carles and Fletcher, 2009; Jeong et al., 2009). However, genome-wide data in *Arabidopsis* did not show a general association between H3K4me3 and H3K27me3 (Ha et al., 2011). Despite previous results (Jiang et al., 2008; Carles and Fletcher, 2009; Jeong et al., 2009), our ChIP experiments did not confirm any significant change for H3K4me3 in the *clf* background either at *FT* or *AG*. An increase for this mark was observed in *swn clf* plants, despite the repression of *FT*. Lafos et al. have recently shown that H3K4me3 levels increase globally in *swn clf* calli, which may explain why higher levels were detected at the *FT* locus (Lafos et al., 2011). In comparison to H3K27 methylation marks, the levels of H3K4me3 at *FT* and *AG* were very low (see Supplemental Figure 3 online), which could explain why the

number of genes that are detected as positive for the H3K4me3 mark genome-wide does not change in mutant seedlings that have lost PRC2 function (Bouyer et al., 2011).

Tissue Differentiation Bypasses Lack of PcG Repression

Considering that chromatin changes are not sufficient to explain *FT* down-regulation in strong PcG mutants and that vascular tissue is the normal domain of *FT* expression, its alteration could be the basis for *FT* down-regulation in *swn clf* callus. Auxin is key to the development of the vascular tissue, and important genes involved in the biosynthesis, transportation, perception, and signaling of this hormone are among PcG targets (Notaguchi et al., 2008; Lafos et al., 2011; Rizzardi et al., 2011). Several genes that play an important role in the auxin pathway are affected in *swn clf* (Figure 3; see Supplemental Data Set 1 online) (Lafos et al., 2011). One possible result of misregulating the auxin pathway is the alteration of vasculature development. This hypothesis is supported by the results in hormone-induced calli and in plants grown in NPA-containing medium. In both situations, the development of the vascular tissue is affected; in hormone-enriched medium by reducing the differentiation of the veins, and in the presence of NPA by increasing the amount and distribution of vascular bundles while impairing their integrity (Figures 5 and 6) (Wenzel et al., 2008). Based on microarray studies performed by the AtGenExpress consortium, neither auxin nor NPA affect *FT* transcription directly (Goda et al., 2008). Therefore, the results confirm the sensitivity of *FT* expression to the appropriate development and differentiation of the vascular tissue. The absence of proper vasculature development prevents the activation of *FT* by CO, which is expressed at normal levels in *swn clf* and is strongly up-regulated in hormone-induced calli.

In summary, our data show that the role of PcG proteins in the regulatory network determining tissue-specific expression is not identical for all PcG-target genes. Although almost one quarter of

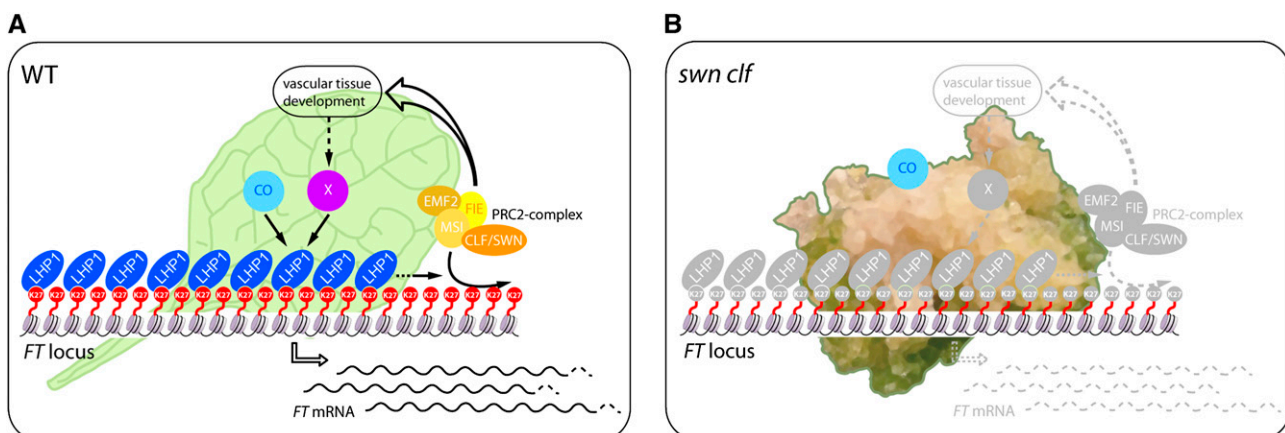


Figure 7. The Impaired Differentiation of Vascular Tissue Bypasses the Lack of PcG Repression.

(A) In a wild-type (WT) leaf, the *FT* expression pattern is the result of the interplay among repressors, such as LHP1 and the PRC2 complex, and activators, such as CO. The PcG pathway is not only involved in the direct repression of *FT* but is also necessary to promote the proper development of the vascular tissue that is essential for *FT* activation through an unknown “X” factor.

(B) In a *swn clf* callus, where the differentiation of the vascular tissue is strongly impaired, CO is not able to activate *FT* expression due to the absence of the vascular “X” factor, despite the loss of PcG repressive marks in the *FT* chromatin.

PcG targets are strongly up-regulated in the *swn clf* mutant (Figure 3) and some have been shown to be ectopically expressed in different PcG mutants (Goodrich et al., 1997; Chanvivattana et al., 2004; Schubert et al., 2006; Calonje et al., 2008; Bratzel et al., 2010), the lack of the repressive H3K27me3 mark is not always synonymous with an increase in the expression domain or increased expression levels. This indicates that the lack of chromatin-mediated repression leads to elevated expression only if additional positive regulators are present. Specifically, the spatial expression of *FT* depends on the proper development and differentiation of the vascular system, and the removal of the PcG-mediated repressive chromatin structure, even in the presence of the activator CO, is not sufficient to overcome this requirement (Figure 7).

METHODS

Plant Materials and Growth Conditions

All the plants used in this work were the Columbia (Col-0) ecotype. *clf-28* (SALK_139371) (Doyle and Amasino, 2009), *swn-7* (SALK_109121), and *swn-7 clf-28* mutants were kindly provided by Daniel Schubert. The *flc-3* mutant has been previously described (Michaels and Amasino, 1999). Due to the sterility of the double mutant, the *8.1kbFT_{prom}:GUS* and *35S:LHP1:HA* transgenic lines (Adrian et al., 2010) were crossed to *swn-7^{-/-} clf-28^{+/-}* and were segregated until plants were obtained carrying each transgene in homozygosis in a *swn-7^{-/-} clf-28^{+/-}* background. The progenies from these lines were analyzed to find the corresponding phenotypes for the wild-type, *clf*, and *swn clf* mutants.

Plants were grown on GM medium under long-day conditions (16 h light/8 h dark) at 20°C. The callus-inducing GM medium was supplemented with 4.5 μM 2,4D and 0.45 μM kinetin (Hu et al., 2000). Overgrowth of the vascular tissue was induced with GM medium supplemented with 10 μM 1-*N*-naphthylphthalamic acid (Wenzel et al., 2008).

Gene Expression Analysis

Total RNA was extracted with the RNeasy mini kit (Quiagen). Five micrograms of RNA were DNase treated using the DNA-free kit (Ambion) to cDNA synthesis. Real time-qPCR was performed using a BioRad iQ5 apparatus and SYBR Green II detection. Expression of *PP2AA3* (At1g13320) (Hong et al., 2010) was used for normalization. Primer sets can be found in Supplemental Table 1 online. GUS staining was performed as previously described (Adrian et al., 2010).

Microarray Analysis and Clustering of Expression Data

For genome-wide distribution of H3K27me3 in the ecotype Col-0, the data set described elsewhere (Göbel et al., 2010; Reimer and Turck, 2010) was used. H3K27me3-positive regions (chers) were determined with the implementation of RINGO (Toedling et al., 2007) in the R package ChIPR (half-window-size: 100, dist_CUT_off:200) and were subsequently mapped to genes according to the TAIR8 genome annotation (minimal number of probes per gene: 3). Genes were considered as H3K27me3 targets if at least 20% of the gene or 500 bp were covered by a positive cher. For microarray expression analysis, total RNA was extracted from 10-d-old Col and *clf-28* and 12-d-old *swn-7 clf-28* seedlings grown on 0.5× MS medium. Affymetrix ATH1 arrays were hybridized with two biological replicates per genotype and processed using the MAS 5.0 procedure (NASARRAYS-425). For each gene, mean fold-change values compared with Col-0 were calculated. Clustering analysis was

performed with all H3K27me3 target genes that were present in the expression data sets (4614 genes).

Clustering was performed with the software Genesis (Sturn et al., 2002). As a distance measurement, the Pearson correlation coefficient was used after computing log₂ fold changes using the wild type as reference. For an overview on the major groups of patterns in the data set, hierarchical clustering was performed on a randomly selected subset of 500 H3K27me3 target genes and revealed eight major groups of expression patterns (see Supplemental Figure 1 online). Therefore, *k* = 8 was used for the K-means clustering analysis shown in Figure 3.

Chromatin Immunoprecipitation

ChIP experiments were performed as previously described (Searle et al., 2006) with anti-H3K27me3 (07-449; Millipore), anti-H3K9me2 (pAb-060-050; Diagenode), anti-H3K27me (pAb-045-050; Diagenode), anti-H3K4me3 (ab1012; Abcam), and anti-HA (H6908; Sigma-Aldrich). A small aliquot of untreated sonicated chromatin was used as the total input DNA. qPCR data were normalized against the input and represented as means of three technical replicates. For background, qPCRs with Ta3 primers were used for H3K27me3, H3K4me3, and LHP1:HA ChIPs, and the average of the signal obtained in each sample was plotted (dashed line in graphs). A similar method was used for H3K9me2 and H3K27me1, but with *RBSC1A* primers (a highly expressed gene) as background measure. Primer sets can be found in Supplemental Table 1 online.

Vascular Staining

Staining of the vasculature was performed by incubating ethanol-clarified plant tissues for 30 min in Basic Fuchsin (0.05%) after 10 min of incubation in 0.2 M NaOH. Excess stain was removed by rinsing in lactic acid.

Immunoblotting

Eleven-day-old *35S_{prom}:CO* (Jang et al., 2008) seedlings were ground in lysis buffer (50 mM MES, pH 8.5, 25 mM KCl, 5 mM MgCl₂, 5% Suc, 30% Glycerol, 10 mM β-mercaptoethanol, 1 mM DTT, 0.3% Triton X-100, 1:1000 Proteinase Inhibitor Cocktail [PIC, Sigma-Aldrich], and 1 mM PMSF). Nuclei were filtered through Miracloth, washed with wash buffer (6 mM MgCl₂, 33 mM KCl, 17 mM HEPES, pH 7.5, 13% Suc, 13% glycerol, 13 mM β-mercaptoethanol, 1 mM DTT, 1.5 mM PMSF, 0.3% Triton X-100, 1:500 PIC), and resuspended in 500 μL Talon buffer (300 mM NaCl, 50 mM NaPO₄, 6 M guanidine HCl, 100 μM ZnSO₄, 100 mM DTT). Proteins were precipitated by addition of ethanol and guanidine to final concentrations of 95% and 0.3 M guanidine, respectively, and were resuspended in 25 μL of resuspension buffer (50 mM Tris HCl, pH 7.5, 150 mM KCl, 10 μM ZnSO₄) and 25 μL of 2× Laemmli buffer. Immunoblots were developed with primary antibodies anti-CO (Valverde et al., 2004) and anti-Histone 3 (ab1791, Abcam) as loading control, and secondary anti-Rabbit IgG-HRPO conjugated (711-035-152, Dianova). The membrane was incubated with a mix of SuperSignal West Dura Chemiluminescent Substrate and SuperSignal West Femto Chemiluminescent Substrate (Pierce Chemical Co.), and the positive signals were detected by a cooled-charge-coupled device camera detection system.

Accession Numbers

Sequence data from this article can be found in the Arabidopsis Genome Initiative data libraries under the following accession numbers: *AG* (At4g18960), *CO* (At5g15840), *FLC* (At5g10140), *FT* (At1g65480), *LHP1* (At5g17690), *SMZ* (At3g54990), *SVP* (At2g22540), *TEM1* (At1g25560), *TEM2* (At1g68840), *CLF* (At2g23380), *SWN* (At4g02020), *VIN3* (At5g57380), *STM* (At1g62360), *RBSC1A* (At1g67090), GSE20256

(Polycomb mutant seedlings microarrays), and E-MTAB-749 (H3K27me3 ChIP-chip data).

Supplemental Data

The following materials are available in the online version of this article.

Supplemental Figure 1. Representative Example of Hierarchical Clustering Based on Expression Data of a Subset of 500 Randomly Selected H3K27me3 Genes.

Supplemental Figure 2. Analysis of *SVP*, *TEM1*, *TEM2*, and *SMZ* Expression in the Wild Type, *clf*, and *swn clf*.

Supplemental Figure 3. LHP1:HA Binding and H3K27me1 Changes at AG and H3K4me3 Changes at FT and AG in the Wild Type, *clf*, and *swn clf*.

Supplemental Figure 4. The Vascular Tissue Loses Its Reticulated Pattern in *swn clf*.

Supplemental Figure 5. CO Protein Is Stable in Hormone-Supplemented Medium.

Supplemental Figure 6. Biological Repeat of Expression Data Presented in Figure 2.

Supplemental Figure 7. Biological Repeat of ChIP Data Presented in Figure 4.

Supplemental Table 1. List of Primers.

Supplemental Data Set 1. Expression Clusters of H3K27me3-Enriched Genes by K-Means Clustering.

ACKNOWLEDGMENTS

We thank Daniel Schubert for providing the PcG mutant lines, Valentina Strizhova and Jesús López-Corrales for excellent technical help, and George Coupland, Wim Soppe, and José C. Reyes for critical reading of the manuscript. We gratefully acknowledge financial support from the Deutsche Forschungsgemeinschaft and the Max Planck Society.

AUTHOR CONTRIBUTIONS

S.F., F.L.T., J.G., and F.T. designed research; S.F., F.L.T., J.A., and L.S.-K. performed research; S.F., F.L.T., J.E., and X.D. analyzed data; and S.F. and F.T. wrote the article.

Received May 28, 2011; revised July 29, 2011; accepted August 29, 2011; published September 13, 2011.

REFERENCES

- Adrian, J., Farrona, S., Reimer, J.J., Albani, M.C., Coupland, G., and Turck, F.** (2010). cis-Regulatory elements and chromatin state coordinately control temporal and spatial expression of FLOWERING LOCUS T in *Arabidopsis*. *Plant Cell* **22**: 1425–1440.
- Aukerman, M.J., and Sakai, H.** (2003). Regulation of flowering time and floral organ identity by a MicroRNA and its APETALA2-like target genes. *Plant Cell* **15**: 2730–2741.
- Barrero, J.M., González-Bayón, R., del Pozo, J.C., Ponce, M.R., and Micol, J.L.** (2007). INCURVATA2 encodes the catalytic subunit of DNA Polymerase alpha and interacts with genes involved in chromatin-mediated cellular memory in *Arabidopsis thaliana*. *Plant Cell* **19**: 2822–2838.
- Bouyer, D., Roudier, F., Heese, M., Andersen, E.D., Gey, D., Nowack, M.K., Goodrich, J., Renou, J.P., Grini, P.E., Colot, V., and Schnittger, A.** (2011). Polycomb repressive complex 2 controls the embryo-to-seedling phase transition. *PLoS Genet.* **7**: e1002014.
- Bratzel, F., López-Torrejón, G., Koch, M., Del Pozo, J.C., and Calonje, M.** (2010). Keeping cell identity in *Arabidopsis* requires PRC1 RING-finger homologs that catalyze H2A monoubiquitination. *Curr. Biol.* **20**: 1853–1859.
- Buzas, D.M., Robertson, M., Finnegan, E.J., and Helliwell, C.A.** (2011). Transcription-dependence of histone H3 lysine 27 trimethylation at the *Arabidopsis* polycomb target gene FLC. *Plant J.* **65**: 872–881.
- Calonje, M., Sanchez, R., Chen, L., and Sung, Z.R.** (2008). EMBRYONIC FLOWER1 participates in polycomb group-mediated AG gene silencing in *Arabidopsis*. *Plant Cell* **20**: 277–291.
- Campos, E.I., and Reinberg, D.** (2009). Histones: Annotating chromatin. *Annu. Rev. Genet.* **43**: 559–599.
- Carles, C.C., and Fletcher, J.C.** (2009). The SAND domain protein ULTRAPETALA1 acts as a trithorax group factor to regulate cell fate in plants. *Genes Dev.* **23**: 2723–2728.
- Castillejo, C., and Pelaz, S.** (2008). The balance between CONSTANS and TEMPRANILLO activities determines FT expression to trigger flowering. *Curr. Biol.* **18**: 1338–1343.
- Chanvivattana, Y., Bishopp, A., Schubert, D., Stock, C., Moon, Y.H., Sung, Z.R., and Goodrich, J.** (2004). Interaction of Polycomb-group proteins controlling flowering in *Arabidopsis*. *Development* **131**: 5263–5276.
- Doyle, M.R., and Amasino, R.M.** (2009). A single amino acid change in the enhancer of zeste ortholog CURLY LEAF results in vernalization-independent, rapid flowering in *Arabidopsis*. *Plant Physiol.* **151**: 1688–1697.
- Exner, V., Aichinger, E., Shu, H., Wildhaber, T., Alfarano, P., Caffisch, A., Grisse, W., Köhler, C., and Hennig, L.** (2009). The chromodomain of LIKE HETEROCHROMATIN PROTEIN 1 is essential for H3K27me3 binding and function during *Arabidopsis* development. *PLoS ONE* **4**: e5335.
- Farrona, S., Coupland, G., and Turck, F.** (2008). The impact of chromatin regulation on the floral transition. *Semin. Cell Dev. Biol.* **19**: 560–573.
- Fisher, C.L., and Fisher, A.G.** (2011). Chromatin states in pluripotent, differentiated, and reprogrammed cells. *Curr. Opin. Genet. Dev.* **21**: 140–146.
- Göbel, U., Reimer, J., and Turck, F.** (2010). Genome-wide mapping of protein-DNA interaction by chromatin immunoprecipitation and DNA microarray hybridization (ChIP-chip). Part B: ChIP-chip data analysis. *Methods Mol. Biol.* **631**: 161–184.
- Goda, H., et al.** (2008). The AtGenExpress hormone and chemical treatment data set: experimental design, data evaluation, model data analysis and data access. *Plant J.* **55**: 526–542.
- Goodrich, J., Puangsomlee, P., Martin, M., Long, D., Meyerowitz, E.M., and Coupland, G.** (1997). A Polycomb-group gene regulates homeotic gene expression in *Arabidopsis*. *Nature* **386**: 44–51.
- Ha, M., Ng, D.W., Li, W.H., and Chen, Z.J.** (2011). Coordinated histone modifications are associated with gene expression variation within and between species. *Genome Res.* **21**: 590–598.
- Hennig, L., and Derkacheva, M.** (2009). Diversity of Polycomb group complexes in plants: Same rules, different players? *Trends Genet.* **25**: 414–423.
- Hong, S.M., Bahn, S.C., Lyu, A., Jung, H.S., and Ahn, J.H.** (2010). Identification and testing of superior reference genes for a starting pool of transcript normalization in *Arabidopsis*. *Plant Cell Physiol.* **51**: 1694–1706.
- Hu, Y., Bao, F., and Li, J.** (2000). Promotive effect of brassinosteroids

- on cell division involves a distinct CycD3-induction pathway in *Arabidopsis*. *Plant J.* **24**: 693–701.
- Imaizumi, T.** (2010). *Arabidopsis* circadian clock and photoperiodism: time to think about location. *Curr. Opin. Plant Biol.* **13**: 83–89.
- Jang, S., Marchal, V., Panigrahi, K.C., Wenkel, S., Soppe, W., Deng, X.W., Valverde, F., and Coupland, G.** (2008). *Arabidopsis* COP1 shapes the temporal pattern of CO accumulation conferring a photoperiodic flowering response. *EMBO J.* **27**: 1277–1288.
- Jeong, J.H., Song, H.R., Ko, J.H., Jeong, Y.M., Kwon, Y.E., Seol, J.H., Amasino, R.M., Noh, B., and Noh, Y.S.** (2009). Repression of FLOWERING LOCUS T chromatin by functionally redundant histone H3 lysine 4 demethylases in *Arabidopsis*. *PLoS ONE* **4**: e8033.
- Jiang, D., Wang, Y., Wang, Y., and He, Y.** (2008). Repression of FLOWERING LOCUS C and FLOWERING LOCUS T by the *Arabidopsis* Polycomb repressive complex 2 components. *PLoS ONE* **3**: e3404.
- Köhler, C., and Hennig, L.** (2010). Regulation of cell identity by plant Polycomb and trithorax group proteins. *Curr. Opin. Genet. Dev.* **20**: 541–547.
- Kwon, C.S., Lee, D., Choi, G., and Chung, W.I.** (2009). Histone occupancy-dependent and -independent removal of H3K27 trimethylation at cold-responsive genes in *Arabidopsis*. *Plant J.* **60**: 112–121.
- Lafos, M., Kroll, P., Hohenstatt, M.L., Thorpe, F.L., Clarenz, O., and Schubert, D.** (2011). Dynamic regulation of H3K27 trimethylation during *Arabidopsis* differentiation. *PLoS Genet.* **7**: e1002040.
- Li, D., Liu, C., Shen, L., Wu, Y., Chen, H., Robertson, M., Helliwell, C.A., Ito, T., Meyerowitz, E., and Yu, H.** (2008). A repressor complex governs the integration of flowering signals in *Arabidopsis*. *Dev. Cell* **15**: 110–120.
- Liu, C., Lu, F., Cui, X., and Cao, X.** (2010). Histone methylation in higher plants. *Annu. Rev. Plant Biol.* **61**: 395–420.
- Mathieu, J., Yant, L.J., Mürdter, F., Küttner, F., and Schmid, M.** (2009). Repression of flowering by the miR172 target SMZ. *PLoS Biol.* **7**: e1000148.
- Michaels, S.D., and Amasino, R.M.** (1999). FLOWERING LOCUS C encodes a novel MADS domain protein that acts as a repressor of flowering. *Plant Cell* **11**: 949–956.
- Notaguchi, M., Abe, M., Kimura, T., Daimon, Y., Kobayashi, T., Yamaguchi, A., Tomita, Y., Dohi, K., Mori, M., and Araki, T.** (2008). Long-distance, graft-transmissible action of *Arabidopsis* FLOWERING LOCUS T protein to promote flowering. *Plant Cell Physiol.* **49**: 1645–1658.
- Ogas, J., Cheng, J.C., Sung, Z.R., and Somerville, C.** (1997). Cellular differentiation regulated by gibberellin in the *Arabidopsis thaliana* pickle mutant. *Science* **277**: 91–94.
- Reimer, J.J., and Turck, F.** (2010). Genome-wide mapping of protein-DNA interaction by chromatin immunoprecipitation and DNA microarray hybridization (ChIP-chip). Part A: ChIP-chip molecular methods. *Methods Mol. Biol.* **631**: 139–160.
- Rizzardi, K., Landberg, K., Nilsson, L., Ljung, K., and Sundås-Larsson, A.** (2011). TFL2/LHP1 is involved in auxin biosynthesis through positive regulation of YUCCA genes. *Plant J.* **65**: 897–906.
- Schubert, D., Primavesi, L., Bishopp, A., Roberts, G., Doonan, J., Jenuwein, T., and Goodrich, J.** (2006). Silencing by plant Polycomb-group genes requires dispersed trimethylation of histone H3 at lysine 27. *EMBO J.* **25**: 4638–4649.
- Schwartz, Y.B., and Pirrotta, V.** (2007). Polycomb silencing mechanisms and the management of genomic programmes. *Nat. Rev. Genet.* **8**: 9–22.
- Searle, I., He, Y., Turck, F., Vincent, C., Fornara, F., Kröber, S., Amasino, R.A., and Coupland, G.** (2006). The transcription factor FLC confers a flowering response to vernalization by repressing meristem competence and systemic signaling in *Arabidopsis*. *Genes Dev.* **20**: 898–912.
- Simon, J.A., and Kingston, R.E.** (2009). Mechanisms of polycomb gene silencing: knowns and unknowns. *Nat. Rev. Mol. Cell Biol.* **10**: 697–708.
- Sturn, A., Quackenbush, J., and Trajanoski, Z.** (2002). Genesis: cluster analysis of microarray data. *Bioinformatics* **18**: 207–208.
- Takada, S., and Goto, K.** (2003). Terminal flower2, an *Arabidopsis* homolog of heterochromatin protein1, counteracts the activation of flowering locus T by constans in the vascular tissues of leaves to regulate flowering time. *Plant Cell* **15**: 2856–2865.
- Tiwari, S.B., et al.** (2010). The flowering time regulator CONSTANS is recruited to the FLOWERING LOCUS T promoter via a unique cis-element. *New Phytol.* **187**: 57–66.
- Toedling, J., Skylar, O., Krueger, T., Fischer, J.J., Sperling, S., and Huber, W.** (2007). Ringo—an R/Bioconductor package for analyzing ChIP-chip readouts. *BMC Bioinformatics* **8**: 221.
- Turck, F., Fornara, F., and Coupland, G.** (2008). Regulation and identity of florigen: FLOWERING LOCUS T moves center stage. *Annu. Rev. Plant Biol.* **59**: 573–594.
- Turck, F., Roudier, F., Farrona, S., Martin-Magniette, M.L., Guillaume, E., Buisine, N., Gagnot, S., Martienssen, R.A., Coupland, G., and Colot, V.** (2007). *Arabidopsis* TFL2/LHP1 specifically associates with genes marked by trimethylation of histone H3 lysine 27. *PLoS Genet.* **3**: e86.
- Valverde, F., Mouradov, A., Soppe, W., Ravenscroft, D., Samach, A., and Coupland, G.** (2004). Photoreceptor regulation of CONSTANS protein in photoperiodic flowering. *Science* **303**: 1003–1006.
- Weinhofer, I., Hehenberger, E., Roszak, P., Hennig, L., and Köhler, C.** (2010). H3K27me3 profiling of the endosperm implies exclusion of polycomb group protein targeting by DNA methylation. *PLoS Genet.* **6**: e1001152.
- Wenzel, C.L., Hester, Q., and Mattsson, J.** (2008). Identification of genes expressed in vascular tissues using NPA-induced vascular overgrowth in *Arabidopsis*. *Plant Cell Physiol.* **49**: 457–468.
- Yamaguchi, A., Kobayashi, Y., Goto, K., Abe, M., and Araki, T.** (2005). TWIN SISTER OF FT (TSF) acts as a floral pathway integrator redundantly with FT. *Plant Cell Physiol.* **46**: 1175–1189.
- Zhang, X., Clarenz, O., Cokus, S., Bernatavichute, Y.V., Pellegrini, M., Goodrich, J., and Jacobsen, S.E.** (2007). Whole-genome analysis of histone H3 lysine 27 trimethylation in *Arabidopsis*. *PLoS Biol.* **5**: e129.

